Steered Spacecraft Deployment Using Interspacecraft Coulomb Forces

Gordon G. Parker, Lyon B. King and Hanspeter Schaub

Abstract— **Recent work has shown that Coulomb forces can be used to maintain fixed-shape formations of spacecraft at high Earth altitudes with practical charging requirements. These formations require a careful balance between the intercraft forces and the relative orbital dynamics. While nearly propellantless, the resulting dynamic equations are nonlinear, and result in a challenging control system design problem. This paper explores a different Coulomb force application where a chief satellite deploys deputy craft to specified end states. By using multiple charge surfaces on the chief, a linear control design approach can be used while guaranteeing reachability for one deputy. This is extended to simultaneous, multiple deputy deployment by modulating control authority across the formation. A 3 deputy example is presented to illustrate the approach where Debye length plasma shielding is considered. This example shows that 1 meter diameter craft can be deployed to a 30 meter, circular projected formation in geostationary orbit in approximately 2 orbits with a maximum of 20 kilovolts on the charge surfaces.**

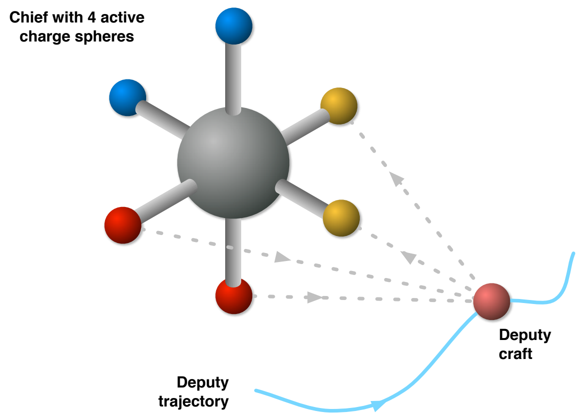

Fig. 1. Steerable Coulomb force deployment scenario. The chief shown has 6 charge spheres, 4 of which are active.

I. INTRODUCTION

The focus of this paper is high Earth orbit (HEO) deployment of relatively small deputy spacecraft using Coulomb forces generated between a chief satellite and the deputies. It is assumed that the chief craft has its own conventional propulsion system, and is in a circular orbit about Earth. Furthermore, the chief has several controllable spherical charge surfaces. The deputy craft are assumed to be spherical, with their own controllable charge capability. Deployment consists of simultaneously repositioning the deputies from an initial configuration near the chief to a specified end-shape, typically multiple chief radii's away. In general, the final speed states of the deputies could be nonzero. During deployment, the deputies react against the chief, exploiting the chief's station keeping capability to generate accurate motions.

A unique feature of Coulomb propulsion is that it requires considerably less propellant than a conventional gas or plasma thruster. In addition, it does not produce contaminating plumes, nor impingement forces. It has also been shown that the power requirements are much less than conventional propulsion systems, even when modulating the charge at relatively high frequency (100s of Hz) [10].

There are several possible uses for Coulomb force deployment. One application is the initial deployment of formation flying spacecraft, with the typical goal being Earth imaging. Related to this is the ability to periodically correct formation flying spacecraft orbits disturbed by external disturbances (e.g. J_2, aerodynamic, solar pressure forces). Deployable and retractable autonomous or semi-autonomous vehicle health monitoring devices is another application. Here the deputies would be used to monitor the chief, with the goal of diagnosing a perceived problem with the chief spacecraft. Finally, because the deputies can be given an end state, including nonzero speed, they could also be used as steerable projectiles.

The use of Coulomb forces for propulsion is a relatively new field. The earliest work examined symmetric, crystal-like structures where one node, the chief, had a conventional propulsion system [4], [8], [9], [10]. This allowed the deputy craft to react against a body that was maintaining a constant orbit. The report in Reference [10] also showed, using data from the SCATHA [11] and ATS [6] missions, that $10\mu N$-$1000\mu N$ level forces could be generated between spacecraft. In addition, charging times were estimated to be in the millesecond range, and the Coulomb 'thrust' propulsion system power consumption was lower than for conventional propulsion methods. More recent work has examined the necessary conditions for static equilibrium where all spacecraft are held together by Coulomb forces alone [13], [12]. Free-flying formations were considered in detail for 2 and 3 spacecraft cases [1]. This was followed by consideration of larger formations using a genetic algorithm optimization strategy to find static shapes for up to 9 spacecrafts [2] where the plasma shielding effect, characterized by the Debye length, was considered negligible.

The remainder of this paper is as follows. The chief and deputy spacecraft dynamic equations are developed in

G. Parker and L. King are with the Department of Mechanical Engineering - Engineering Mechanics, Michigan Technological University, Houghton, MI 49931, USA ggparker@mtu.edu

H. Schaub is with the Department of Aerospace and Ocean Engineering, Virginia Polytechnic Institute and State University, Blacksburg, VA 24091, USA hschaub@vt.edu

Section II. The control strategy is presented in Section III starting with 1 deputy, and then extending it to N deputies. Conditions for chief charge sphere locations are also discussed. Section IV illustrates the approach with an example where the chief has 4 charge spheres, and there are 3 participating deputies. A few concluding remarks are provided in Section V, along with plans for future work.

II. DYNAMIC MODEL

Before examining the formation dynamic equations, the Coulomb charge, voltage and force relationships should be discussed.

It's well known that Coulomb forces exist between charged bodies. Considering the two homogeneously charged spheres of Fig. 2 the Coulomb force magnitude acting on body 1, directed along the line between the spheres is

$$f_{12} = \frac{k_c q_1 q_2}{d^2} \tag{1}$$

where k_c is Coulomb's constant ($8.99 \times 10^9 \frac{Nm^2}{C^2}$), q_1 and q_2 are the sphere charges in Coulombs and d is the distance between the center of the spheres in meters.

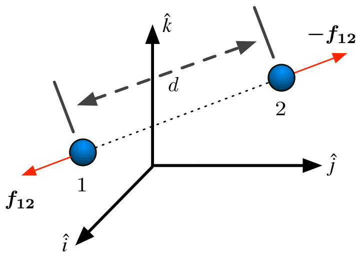

Fig. 2. Coulomb forces between two spheres having the same charge sign.

An important deviation from the ideal Coulomb force model of (1) occurs when considering charged bodies in a plasma-rich environment, as found in space. In short, the plasma shields the Coulomb force effect exponentially with the separation distance as shown in (2). The exponential decay of the Coulomb force is characterized by the Debye length, λ_d, which varies with plasma characteristics [3]. In general, the Debye length is small at LEO and large at HEO (roughly 10 cm and 100 m respectively)

$$f_{12} = \frac{k_c q_1 q_2}{d^2} e^{-d/\lambda_d}. \tag{2}$$

When charged spacecraft are more than 2 Debye length apart, then their Coulomb force interaction becomes negligible for realistic charge scenarios. Finally, it should be noted that the charges can be converted to voltages for the ith craft, which may give more practical insight, according to

$$V_i = \frac{q_i k_c}{r_n} \tag{3}$$

where r_n is the radius of the spherical charge device.

Next, Hill's equations [7] (also known as the Clohessy-Wiltshire equations, [5]) are used to generate the formation dynamic equations for the Coulomb controlled system. Consider a system consisting of N_d deputy craft, and a chief containing N_c charge points. The specific case of 3 deputies and 1 charge sphere is shown in Fig. 3. The position vectors of the $N_d + N_c$ bodies are ordered such that $\boldsymbol{p}_1$ through $\boldsymbol{p}_{N_d}$ are the deputy vectors and $\boldsymbol{p}_{N_d+1}$ through $\boldsymbol{p}_{N_d+N_c}$ are the charge sphere vectors, all relative to the center of the chief satellite. Each position vector has elements x_i, y_i and z_i. Referring to the example of Fig. 3, the 3 deputy craft position vectors are denoted $\boldsymbol{p}_1$ through $\boldsymbol{p}_3$ and the chief's charge sphere position vector is denoted $\boldsymbol{p}_4$. The chief is assumed to be in a circular orbit about the Earth with a Hill coordinate frame at its center as shown in Fig. 3. The $\hat{i}$ unit vector is pointing radially outward from the center of the Earth and the $\hat{j}$ axis is in the direction of the chief's velocity vector. Each of the $N_d + N_c$ bodies is assumed to have charge q_i.

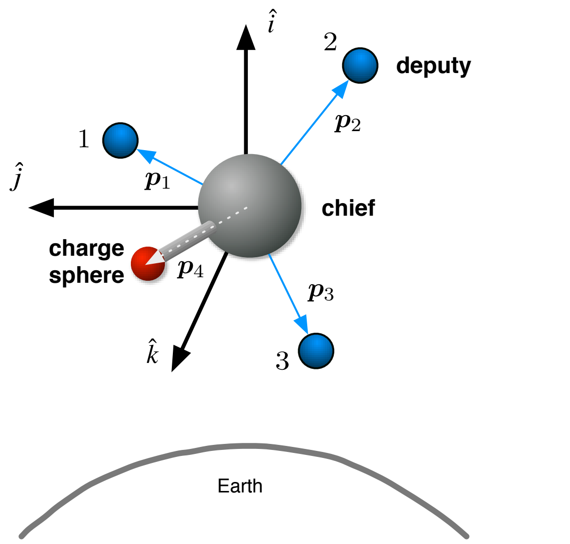

Fig. 3. Three virtual structure nodes orbiting the Earth illustrating the notation used in the model development.

Applying the Coulomb forces to the right side of Hills Equations, yields the system dynamic equations for small motions about the chief satellite and are shown in (4)

$$\begin{aligned} m\left(\ddot{x}_i - 2n\dot{y}_i - 3n^2 x_i\right) &= k_c \sum_{j=1}^{N_d+N_c} \frac{x_i - x_j}{d_{ij}^3} q_i q_j e^{-\frac{d_{ij}}{\lambda_d}} \\ m\left(\ddot{y}_i + 2n\dot{x}_i\right) &= k_c \sum_{j=1}^{N_d+N_c} \frac{y_i - y_j}{d_{ij}^3} q_i q_j e^{-\frac{d_{ij}}{\lambda_d}} \\ m\left(\ddot{z}_i + n^2 z_i\right) &= k_c \sum_{j=1}^{N_d+N_c} \frac{z_i - z_j}{d_{ij}^3} q_i q_j e^{-\frac{d_{ij}}{\lambda_d}} \end{aligned} \tag{4}$$

for $i = 1 \ldots N_d$, $j \neq i$ during the summation and $d_{ij} = \|\boldsymbol{p}_i - \boldsymbol{p}_j\|$. The Hill frame angular velocity is denoted as n and the mass of each deputy is m. Equation (4) is nonlinear and results in a challenging control problem if the goal is to simultaneously move the deputies from initial positions near the chief to final states away from the chief. When all the deputies are charged, the $q_i q_j$ terms limit the ability to create arbitrary force vector directions. Furthermore, as the craft move away from each other and the chief, the Debye length effect exponentially reduces the force capability. It should be noted that the Debye length λ_d can be as little as 10 cm at low altitudes. Therefore, the ability to generate Coulomb forces between craft at large distances is impractical. However, imparting large initial velocities is still quite feasible. At high altitudes, such as geostationary orbit (35,800 km, $n = 7.28 \times 10^{-5}\text{rad/sec}$), λ_d varies from 75 m to 575 m. Thus, long-distance positioning capability is possible.

III. CONTROL STRATEGY

The movement of one deputy is considered first, followed by the extension to multiple deputies. For the single deputy case, $N_d = 1$, (4) becomes

$$\begin{aligned} m\left(\ddot{x}_1 - 2n\dot{y}_1 - 3n^2 x_1\right) &= k_c \sum_{j=2}^{1+N_c} \frac{x_1 - x_j}{d_{1j}^3} q_1 q_j e^{-\frac{d_{1j}}{\lambda_d}} \\ m\left(\ddot{y}_1 + 2n\dot{x}_1\right) &= k_c \sum_{j=2}^{1+N_c} \frac{y_1 - y_j}{d_{1j}^3} q_1 q_j e^{-\frac{d_{1j}}{\lambda_d}} \\ m\left(\ddot{z}_1 + n^2 z_1\right) &= k_c \sum_{j=2}^{1+N_c} \frac{z_1 - z_j}{d_{1j}^3} q_1 q_j e^{-\frac{d_{1j}}{\lambda_d}} \end{aligned} \quad (5)$$

where $d_{1j} = \|\boldsymbol{p_1} - \boldsymbol{p_j}\|$. Assume that the charge of the deputy, q_1, is held to some nonzero, constant value and that $N_d = 3$. Next, denote the right sides of each equation in (5), specifiable forces, using the variables $f_{d,x}, f_{d,y}$, and $f_{d,z}$, or in vector form, $\boldsymbol{f}_d$. As long as the rank of the matrix

$$\boldsymbol{P} = \left[(\boldsymbol{p}_1 - \boldsymbol{p_2}) \quad (\boldsymbol{p}_1 - \boldsymbol{p_3}) \quad \dots \quad (\boldsymbol{p}_1 - \boldsymbol{p}_{1+N_d})\right] \quad (6)$$

is 3, then any desired force, $\boldsymbol{f}_d$, can be applied to the deputy. Because it is possible to generate any force vector, it is clear that a suitable control law can now be applied depending on the application (e.g. tracking, regulation, etc.). For example, a simple proportional controller with rate feedback and orbital dynamics cancellation is suitable for moving the deputy from some initial point to a final point with zero final speed

$$\boldsymbol{f}_d = \begin{Bmatrix} -2n\dot{y}_1 - 3n^2 x_1 \\ 2n\dot{x}_1 \\ n^2 z_1 \end{Bmatrix} + \boldsymbol{K_p}\left(\boldsymbol{p}_{1d} - \boldsymbol{p}_1\right) - \boldsymbol{K_d}\dot{\boldsymbol{v}}_1 \quad (7)$$

where $\boldsymbol{K_p}$ and $\boldsymbol{K_d}$ are 3×3 diagonal gain matrices, $\boldsymbol{p}_{1d}$ is the desired final position of the deputy, and $\boldsymbol{v}_1$ is the velocity of the deputy.

At this point, it is convenient to rewrite the right side of (5) as $\boldsymbol{f}_d = \boldsymbol{Bq}$ where the j^{th} column of the $3 \times N_c$ matrix $\boldsymbol{B}$ is

$$\boldsymbol{B}_j = k_c\left(\boldsymbol{p}_1 - \boldsymbol{p}_j\right) \cdot \left(\frac{e^{-\frac{d_{1j}}{\lambda_d}}}{d_{1j}^3}\right) q_1 \quad (8)$$

and the $N_d \times 1$ vector of inputs, $\boldsymbol{q}$, is

$$\boldsymbol{q} = \begin{Bmatrix} q_2 \\ q_3 \\ \vdots \\ q_{(1+N_d)} \end{Bmatrix}. \quad (9)$$

Some comments on the number of chief charge spheres is in order. If $N_c = 3$, the charge spheres form a plane and defines a singular region where forces orthogonal to the plane cannot be achieved. Thus, a minimum of 4 charge spheres is needed to guarantee complete maneuverability of the deputy. This introduces redundancy in the control law solution. This could be handled by switching between sets of 3 charge spheres, or by utilizing all the charge sphere assets according to some optimization criteria. In this work, a weighted least squares solution is used. Specifically, given the desired force vector to be applied to the debuty, $\boldsymbol{f}_d$, the charge sphere charge values are computed according to

$$\boldsymbol{q} = \boldsymbol{W}^{-1}\boldsymbol{B}^T\left(\boldsymbol{B}\boldsymbol{W}^{-1}\boldsymbol{A}^T\right)^{-1}\boldsymbol{f}_d \quad (10)$$

where $\boldsymbol{W}$ is an $N_c \times N_c$ matrix of constants used to focus control authority onto specific charge spheres. The identity matrix is used in the example below.

Extending this method to multiple deputies can be accomplished in several ways. One approach is to move each deputy to its final state sequentially. In some applications, this may be appropriate. However, if the goal is to have all the deputies be at their goal points at the same time, this would not be suitable. The orbital dynamics quickly result in a loss of positioning accuracy once the Coulomb force is removed and the deputies move according to their own Keplarian motion. The method used in this work is to focus control sequentially between the participating deputies. For example, the formation control period, denoted ΔT, would be divided into N_d equal pieces as $\delta T = \Delta T / N_d$. During each δT only 1 deputy is charged, and the solution to (10) is formed with a $\boldsymbol{B}$ matrix where the $\boldsymbol{p_1}$ of (8) is replaced with i for the i^{th} deputy. It should be noted that from a practical perspective, this assumes that: (1) the deputy charges can be cycled from zero to the maximum value at least 10 times faster than δT, (2) the chief and deputies have a communication protocol that allows the chief to designate which deputy is under control, (3) the chief can measure the deputy position vectors.

IV. EXAMPLE

Three deputies are considered, $N_d = 3$, and 6 charge spheres, $N_c = 6$. The goal is to move the deputies from their initial locations, near the chief, to a final zero speed state such that they lie on a circle, as viewed from Earth, with a radius of 30 meters. The deputies and charge sphere radii are all 0.5 meters, each with a mass of 50 kg. The initial and final coordinates of the deputies are given in Table I along with the coordinates of the charge spheres where $L_i = 3/\sqrt{2}$, $L_f = 30$, and $L_c = 2$. The Debye length is assumed to be 100 meters, and the altitude of the chief is 35,800 km (the orbital period is 24 hours). The time that each deputy is being controlled by the chief's charge spheres is $\delta T = 5$ minutes and the piece-wise constant charge of the deputies is 20,000 volts.

Fig. 4 shows the trajectories of all three deputies - blue for $\boldsymbol{p}_1$, green for $\boldsymbol{p}_2$ and red for $\boldsymbol{p}_3$. The hollow circles indicate the initial positions and the filled circles the end

TABLE I

INITIAL AND FINAL COORDINATES OF THE DEPUTY CRAFT, AND THE COORDINATES OF THE CHARGE SPHERES.

Position Vector	x (m)	y (m)	z (m)
Initial $\boldsymbol{p}_1$	0	L_i	L_i
Initial $\boldsymbol{p}_2$	0	$-L_i$	$-L_i$
Initial $\boldsymbol{p}_3$	0	$-L_i$	L_i
Final $\boldsymbol{p}_1$	0	$\frac{1}{2}L_f$	$\frac{1}{2\sqrt{3}}L_f$
Final $\boldsymbol{p}_2$	0	0	$-\frac{1}{\sqrt{3}}L_f$
Final $\boldsymbol{p}_3$	0	$-\frac{1}{2}L_f$	$\frac{1}{2\sqrt{3}}L_f$
$\boldsymbol{p}_4$	L_c	0	0
$\boldsymbol{p}_5$	$-L_c$	0	0
$\boldsymbol{p}_6$	0	L_c	0
$\boldsymbol{p}_7$	0	$-L_c$	0
$\boldsymbol{p}_8$	0	0	L_c
$\boldsymbol{p}_9$	0	0	$-L_c$

points. The charge spheres are not shown. The only care taken in selecting the initial and end points was to inhibit significant x-axis motion. This was done merely to create an example that could be viewed easily on a two-dimensional plot. As seen in Fig. 4 the motion in the x direction is small compared to the y and z motion.

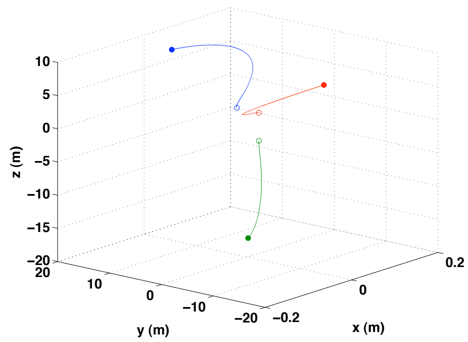

Fig. 4. Trajectories of all three deputies. The hollow circles are the initial configuration, and the filled circles the final positions.

Fig. 5 shows the charge spheres, black circles, and the trajectories of the deputy spacecraft. Again, blue denotes $\boldsymbol{p}_1$, green denotes $\boldsymbol{p}_2$, and red denotes $\boldsymbol{p}_3$. The hollow black sphere at the origin indicates the location of the $\boldsymbol{p}_4$ and $\boldsymbol{p}_5$ charge spheres and are outside the $y-z$ plane. As expected from the control strategy, the motion of the deputies is in a straight line to their respective goals since the desired force vector, $\boldsymbol{f}_d$ is always pointed from the deputy toward its goal. This feature may be useful in the future for path planning.

Fig. 6 shows the x, y, and z coordinates for each deputy. The x motion is a dotted line, the y motion a solid line, and the z motion a dashed line in all cases. From this view it is clear that the deputies achieve their final end points in approximately 2 orbits (2 days).

Voltage time histories are shown in Fig. 7 and Fig. 8. These were computed from the charges, q_i, using (3). It's clear that the maximum voltage required is approximately 20 kilovolts. It should be noted that since the current requirements are

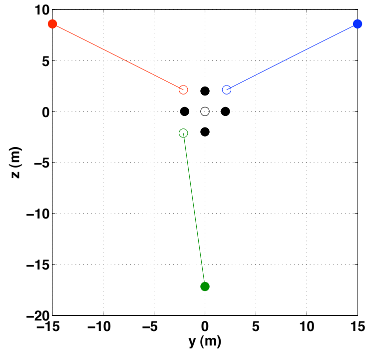

Fig. 5. Trajectories of all three deputies projected onto the $y-z$ plane. Hollow circles are the initial positions, and the filled circles the final positions.

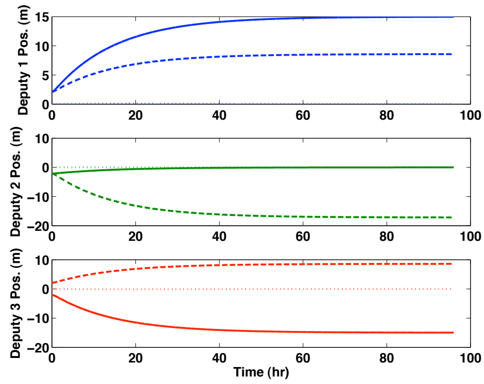

Fig. 6. Time histories of all three deputies where in each plot the dotted line is the x coordinate, the solid line is the y coordinate, and the dashed line is the z coordinate.

extremely small, this requires very little power compared to conventional thrusters. The oscillatory nature of these time histories is due to the switching, every 5 minutes, of the control objective to a different deputy. This is seen more clearly in the "zoomed view" of the $\boldsymbol{p}_4$ charge sphere shown in Fig. 9. It should be noted that the steady-state part of Fig. 7 and Fig. 8, after about 50 hours, is keeping the deputies at the desired fixed positions, constantly working to overcome the orbital forces.

V. CONCLUSIONS AND FUTURE WORK

A. Conclusions

A method was developed for Coulomb control positioning of deputy spacecraft using charged spheres attached to a chief satellite. By focusing on one deputy at a time, a linear control solution was applied to a single deputy. This was extended to simultaneous movement of all the deputies by cycling the charge between deputies. The requirement for the existence of a control solution was given in (6). In practice one should plan the trajectories such that the deputies do not need to cross through the volume bounded by the charge spheres. This is not a very restrictive constraint, and means that the deputies should be moving outward from the chief.

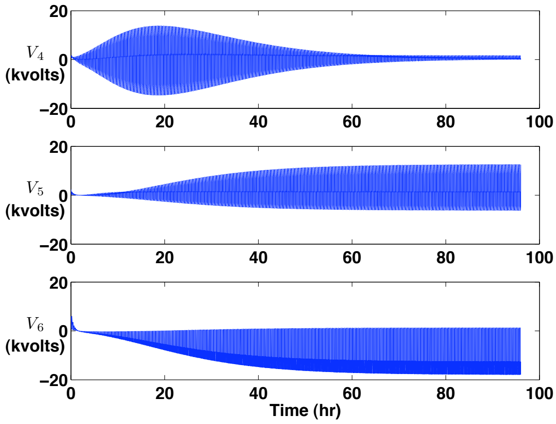

Fig. 7. Charge sphere voltage time histories for spheres 4,5, and 6.

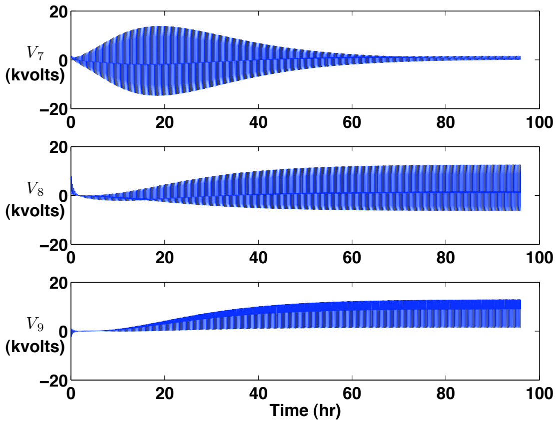

Fig. 8. Charge sphere voltage time histories for spheres 7,8, and 9.

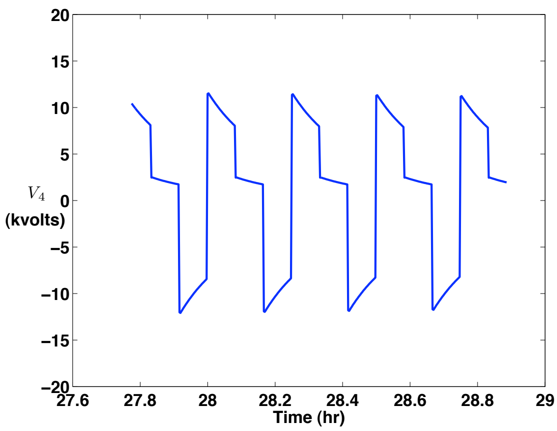

Fig. 9. Zoomed view of charge sphere 4 showing the control authority switching.

B. *Future Work*

There are numerous areas for further study in the general area of Coulomb controlled formations. Related more specifically to the method described in this paper, certainly stability of the modulated control solutions needs to be examined. The ability to generate desired trajectories, not just end points, that exploit the orbital dynamics would also be helpful. Coulomb force attitude control is another area that could benefit from this approach.

VI. ACKNOWLEDGMENTS

This work was supported by the U.S. Defense Advance Research Projects Agency (DARPA), Special Projects Office (SPO) under contract number HR0011-05-C-0026. Approved for public release with unlimited distribution.

REFERENCES

[1] J. Berryman and H. Schaub, "Analytical charge analysis for 2- and 3-craft coulomb formations," in *AAS/AIAA Astrodynamics Specialist Conference*, Lake Tahoe, CA, August 7–11 2005, paper No. AAS 05–278.

[2] ——, "Static equilibrium configurations in geo coulomb spacecraft formations," in *AAS Spaceflight Mechanics Meeting*, Copper Mountain, CO, Jan. 23–27 2005, paper No. AAS 05–104.

[3] F. F. Chen, *Plasma Physics and Controlled Fusion Volume 1: Plasma Physics*. Plenum Press, 1984, ch. 1.

[4] J.-H. Chong, "Dynamic behavior of spacecraft formation flying using coulomb forces," Master's thesis, Michigan Technological University, 2002.

[5] W. H. Clohessy and R. S. Wiltshire, "Terminal guidance system for satellite rendezvous," *Journal of the Aerospace Sciences*, vol. 27, no. 9, pp. 653–658, September 1960.

[6] H. B. Garrett and S. E. DeFrost, "An analytical simulation of the geosynchronous plasma environment," *Planetary Space Science*, vol. 27, pp. 1101–1109, 1979.

[7] G. W. Hill, "Researches in the lunar theory," *American Journal of Mathematics*, vol. 1, no. 1, pp. 5–26, 1878.

[8] L. B. King, G. G. Parker, and J.-H. Chong, "Coulomb controlled spacecraft formation flying," *AIAA Journal of Propulsion and Power*, vol. 19, no. 3, pp. 497–505, 2003.

[9] L. B. King, G. G. Parker, S. Deshmukh, and J.-H. Chong, "A study of inter-spacecraft coulomb forces and implications for formation flying," in *38th AIAA/ASME/SAE/ASEE Joint Propulsion Conference and Exhibit*. Indianapolis, IN: AIAA Paper No. 2002-3671, July 2002.

[10] ——, "Spacecraft formation-flying using inter-vehicle coulomb forces," NASA Institute for Advanced Concepts, http://www.niac.usra.edu/studies, Tech. Rep., 2002. [Online]. Available: http://www.niac.usra.edu/studies/

[11] E. G. Mullen, M. S. Gussenhoven, and D. A. Hardy, "Scatha survey of high-voltage spacecraft charging in sunlight," *Journal of the Geophysical Sciences*, vol. 91, pp. 1074–1090, 1986.

[12] H. Schaub, C. Hall, and J. Berryman, "Necessary conditions for circularly-restricted static coulomb formations," in *AAS Malcolm D. Shuster Astronautics Symposium*, Buffalo, NY, June. 12–15 2005, paper No. AAS 05–472.

[13] H. Schaub, G. G. Parker, and L. B. King, "Challenges and prospects of coulomb satellite formation flying," in *AAS John L. Junkins Astrodynamics Symposium*. College Station, TX: AAS Paper No. AAS03-278, May 2003.